

Supporting Information

Effect of Backbone Chemistry on the Structure of Polyurea Films Deposited by Molecular Layer Deposition

David S. Bergsman[†], Richard G. Closser[‡], Christopher J. Tassone^{||}, Bruce M. Clemens[#], Dennis Nordlund^{||}, and Stacey F. Bent^{†*}

[†]Department of Chemical Engineering, [‡]Department of Chemistry, [#]Department of Materials Science and Engineering, Stanford University, Stanford, California 94305, United States. ^{||}SLAC National Accelerator Laboratory, Menlo Park, California 94025, United States.

Deposition Conditions

MLD growth began with a dose of diisocyanate monomer (PDIC or BDIC) before purging with nitrogen gas, dosing a diamine monomer (ED, BD, or PD), and purging with nitrogen gas again. Repetitions of this process were performed until a desired number of cycles were completed. Dosing was controlled by diaphragm valves purchased from Swagelok, which were operated by LabVIEW software. Each monomer was dosed with the pump closed off to the reactor for a set period of time (open time), before closing the precursor valve and allowing the monomer vapor to stay in the reactor for an additional period of time (pulse time). The reactor was then purged with N₂ with the pump open before starting the next cycle. Dosing conditions varied between reactions and reactors due to differences in reactivity of the chemistries and flow conditions in the reactors: PDIC+PD, PDIC+ED, PDIC+BD, BDIC+ED, and BDIC+BD used open times of 900/900 s, 600/0.5 s, 900/2 s, 20/0.2 s, and 150/2 s, pulse times of 0/0 s, 0/120 s, 0/900 s, 800/120 s, and 600/600 s, and purge times of 600/1200 s, 720/720 s, 600/600 s, 2400/1500 s, and 1200/1200 s, respectively (in this notation, A/B represents the time for the A and B monomers respectively). Sequence times were chosen to ensure sufficient reaction time and purge time for complete saturated growth behavior. Complete saturation curves were not taken for all the chemistries due to the experimentally impractical number of additional runs required. However, full saturation curves were obtained for the PDIC+ED chemistry previously¹ and saturation conditions were confirmed for the other chemistries by doubling the purge and reaction times to confirm that no changes in growth rate took place.

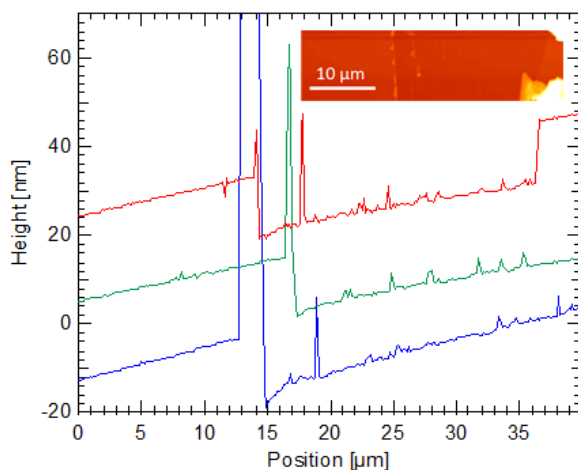
Verification of Ellipsometry Model using Scratch Test

In order to verify that the ellipsometry model was accurately capturing the thickness of films, a combination of an atomic force microscopy (AFM) scratch test and X-ray reflectivity (XRR) were performed for each of the chemistries.

For the AFM scratch test, films of each of the chemistries were scratched in three different locations on the sample by applying light pressure with Teflon-coated tweezers across the wafer. The samples were then examined using AFM on a Park XE-70 atomic force microscope in non-contact mode with ACTA 10M tips purchased from Park Systems (thickness 4 μm).

AFM scans of size 40 x 40 μm were taken over the scratched areas to produce a line profile (see Supplemental Figure 1). The change in height between a line fit of the scratched and unscratched areas was used to represent the film thickness. The resulting film thicknesses measured by AFM compared to the thicknesses measured by ellipsometry are shown in Supplemental Table 1 below.

During this process, it was found that the BDIC+BD chemistry was particularly difficult to remove by scratching, likely due to the relative thinness of the samples deposited using this chemistry and the relatively increased degree of crystallinity. Thus, additional scratches (a total of 7) were made for this BDIC+BD chemistry in order to smooth out the greater fluctuations in film thickness, which is represented in the relative uncertainty of the measurement.

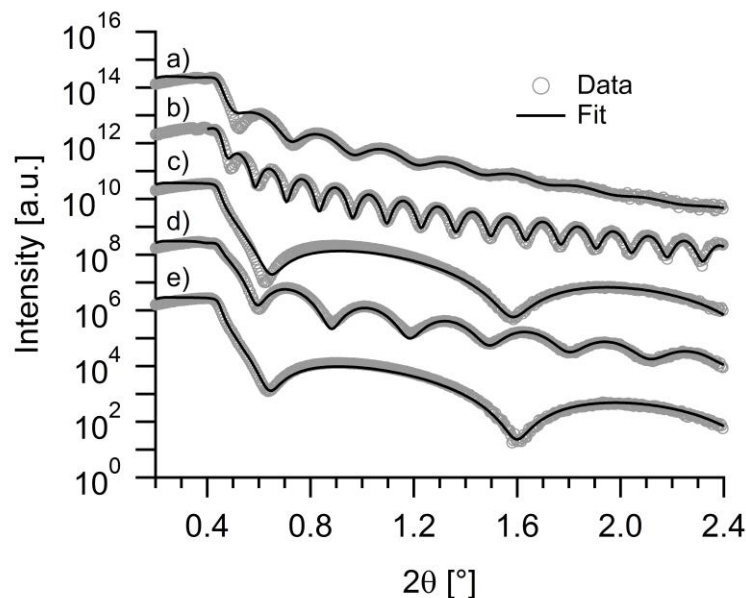


Supplemental Figure 1: Example AFM line scans from scratching a PDIC+BD film. Inset shows a micrograph of one of the scratches.

Supplemental Table 1: Comparison of thicknesses measured by ellipsometry and AFM for each of the chemistries explored.

Chemistry	Thickness (Ellipsometry)	Thickness (AFM)
(PDIC+PD)	14.3 nm	15.4 ± 0.4 nm
(PDIC+ED)	23.7 nm	24.1 ± 1.8 nm
(PDIC+BD)	12.3 nm	12.3 ± 0.5 nm
(BDIC+ED)	5.8 nm	5.4 ± 0.6 nm
(BDIC+BD)	2.9 nm	3.1 ± 1.1 nm

For the XRR experiments, films of each of the chemistries were examined ex situ using a PAN Analytical X'pert Materials Research Diffractometer with Cu K α radiation ($\lambda=1.54 \text{ \AA}$) and fit using the provided PAN Analytical X-ray reflectivity software using a Si/SiO $_x$ /MLD film model. The data and resulting fits are shown in Supplemental Figure 2 below, along with a table summarizing the resulting fits for film thickness, density of the films, and comparable film thickness measured with ellipsometry (Supplemental Table 2).



Supplemental Figure 2: XRR for each of the chemistries studied: a) PDIC+PD, b) PDIC+ED, c) PDIC+BD, d) BDIC+ED, and e) BDIC+BD. All peaks except for (e) are shifted for ease of viewing.

Supplemental Table 2: Comparison of thicknesses measured by ellipsometry and XRR for each of the chemistries explored, as well as the fit film densities.

Chemistry	Thickness (Ellipsometry)	Thickness (XRR)	Density (XRR)
(PDIC+PD)	32.7 nm	33.7 nm	0.96 g/cm ³
(PDIC+ED)	63.2 nm	63.5 nm	1.17 g/cm ³
(PDIC+BD)	7.1 nm	8.6 nm	1.28 g/cm ³
(BDIC+ED)	25.2 nm	27.4 nm	1.17 g/cm ³
(BDIC+BD)	7.1 nm	8.8 nm	1.28 g/cm ³

NEXAFS Measurement Conditions

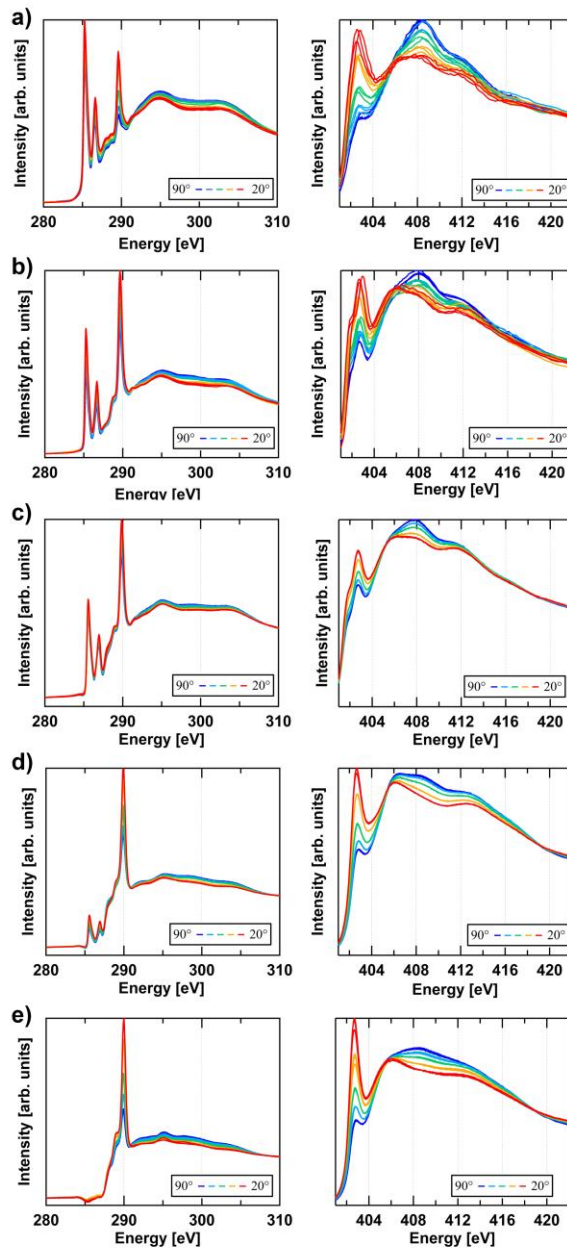
Angle-dependent NEXAFS measurements were performed using a spherical grating monochromator operated at 0.2 eV resolution and an approximately 0.5x0.5 mm² beam foot print. A linear p-polarization of 0.88 was assumed, based on previous measurements performed at the beamline. Spectral intensities were normalized for incoming flux variations using a mesh with evaporated gold positioned upstream of the beam. The sample drain current was used to measure the Total Electron Yield (TEY). The relative energy scale of all the C1s XAS spectra were corrected using the “i0 dip” of the gold mesh and then an absolute shift was applied to all spectra such that the core-exciton peak from a freshly cleaved substrate of highly-ordered pyrolytic graphene² was aligned at 291.65 eV. The energy scale of the N 1s spectra were corrected by aligning the main π^* peak associated with the urea functionality of the PDIC based polymers to the published value of 402.7 eV from gas-phase N-phenyl urea collected by Urquhart et al using electron energy loss spectroscopy³. A linear background was subtracted by linear regressions in the 260-280 eV region for carbon K-edge spectra and the 390-396 eV region for the nitrogen K-edge

spectra. The spectra were normalized at higher energy (320-340 eV and 430-440 eV, respectively) while retaining a constant area in the regions between 280-320 eV and 396-420 eV.

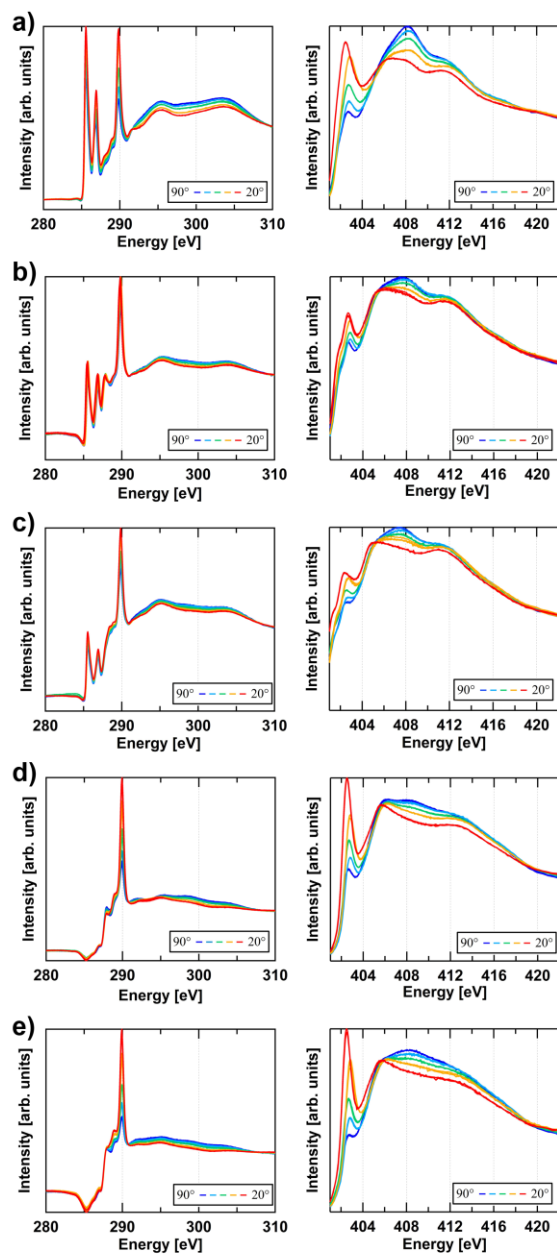
The energy positions of the peaks were guided by the difference spectra between the grazing and normal x-ray incidence spectra. Step functions were positioned for each unique atomic site based on previous measurements of the binding energies previously measured for the PDIC+ED chemistry¹ and their relative intensities were set to be proportional to their atomic fractions. The orientation of the C-N bond was specifically determined using the $\sigma_{\text{C-N}}$ and $\sigma_{\text{N-C}}$ bond orientations, which were assumed to be composed of a roughly linear C-N-C-N-C series (the linear carbon-nitrogen bonds in urea) based on the work of Hähner et al.⁴ and the difficulty of fitting a building block model-type molecular orbital, which has been observed previously⁵.

NEXAFS Plots

The complete NEXAFS spectra for the bulk and thin film chemistries are shown Supplemental Figures 3 and 4. Bulk measurements used 24 cycles of PDIC+PD, 45 cycles of PDIC+ED, 32 cycles of PDIC+BD, 48 cycles of BDIC+ED, and 32 cycles of BDIC+BD. Thin film measurements used 4 cycles of PDIC+PD, 4 cycles of PDIC+ED, 4 cycles of PDIC+BD, 8 cycles of BDIC+ED, and 4 cycles of BDIC+BD.

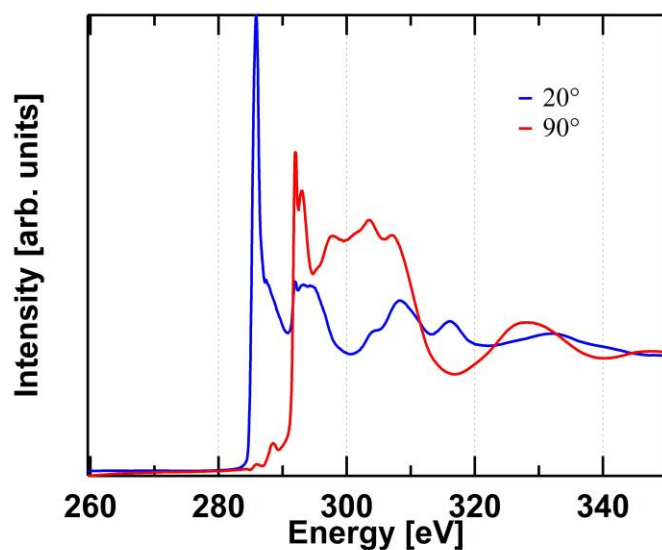


Supplemental Figure 3: Angle-dependent C 1s (left) and N 1s (right) NEXAFS spectra for a) 24x[PDIC+PD], b) 32x[PDIC+BD], c) 45x[PDIC+ED], d) 48x[BDIC+ED], e) 32x[BDIC+BD].



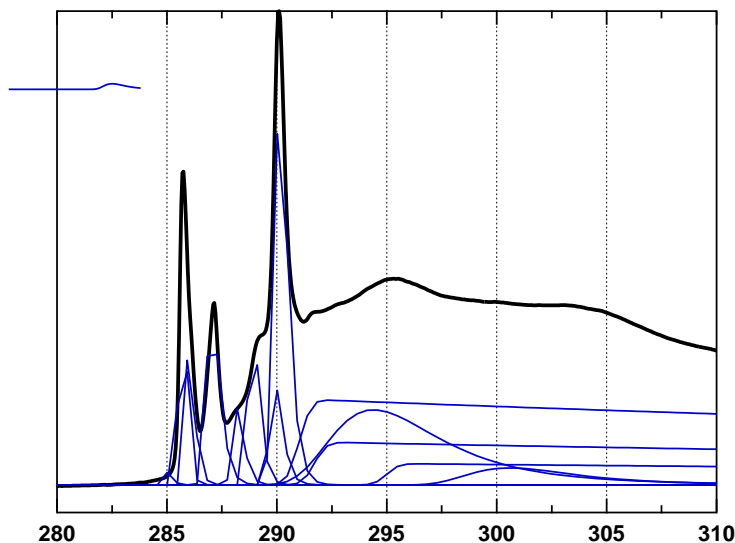
Supplemental Figure 4: Angle-dependent C 1s (left) and N 1s (right) NEXAFS spectra for a) 4x[PDIC+PD], b) 4x[PDIC+BD], c) 4x[PDIC+ED], d) 8x[BDIC+ED], e) 4x[BDIC+BD].

In order to verify the energy positions of the spectra, a comparison was made to the energy of the carbon exciton of highly ordered pyrolytic graphene.



Supplemental Figure 5: NEXAFS spectra of HOPG sample at both grazing and normal X-ray incidence after the core-exciton peak was aligned to 291.65 eV.

Each of the different chemistries was fit using a different set of assigned step edges and Gaussian peaks. An example of this is shown in Supplemental Figure 6 below, which demonstrates one such fit.



Supplemental Figure 6: Example NEXAFS fit.

Though peak fittings were performed on the entire spectra, primary attention was given to peaks with well-resolved assignments, such as the two $C1s \rightarrow 1\pi^*_{C=C}$ resonance, the $C1s \rightarrow 1\pi^*_{C=O}$ resonance, the relative intensities and positions of the step edges, and the $C1s \rightarrow 1\sigma^*_{C=C}$, $C1s \rightarrow 1\sigma^*_{C=C}$, and $C1s \rightarrow 1\sigma^*_{C=O}$ resonances. Mixed features in between these were fit with unobtrusive peaks to allow for accurate fitting of the primary peaks of interest.

Tables for each of the peak positions and widths are shown in the tables below for the reader's perusal.

Supplemental Table 3: C1s Peak Assignments for PDIC+PD Chemistry

Assignment	$(\text{C-C})_{\text{ring}} \rightarrow \pi^*$	$\text{C=O} \rightarrow \pi^*$	$(\text{C-C})_{\text{ring}} \text{ Step}$	C-N Step	C=O Step	$\text{C-C} \rightarrow \sigma^*$	$\text{C-N} \rightarrow \sigma^*$	$\text{C=O} \rightarrow \sigma^*$
Position [eV]	285.43	289.64	290.6	291.3	294.6	294	300.2	303.15
Width [eV]	2.95	4.48	1	1	1	22.80	22.00	22.10
Exp. decay	0.3	0.32	0.01	0.01	0.01	0.5	0.5	0.5

Supplemental Table 4: N1s Peak Assignments for PDIC+PD Chemistry

Assignment	$\text{N-C} \rightarrow \pi^*$	N-C Step	$\text{N-C} \rightarrow \sigma^*$
Position [eV]	402.7	404.93	408.31
Width [eV]	10.24	1	12.26
Exp. decay	0.3	0.017	0.6

Supplemental Table 5: Peak Assignments for PDIC+ED Chemistry

Assignment	$(\text{C-C})_{\text{ring}} \rightarrow \pi^*$	$\text{C=O} \rightarrow \pi^*$	$(\text{C-C})_{\text{ring}} \text{ Step}$	C-N Step	C=O Step	$\text{C-C} \rightarrow \sigma^*$	$\text{C-N} \rightarrow \sigma^*$	$\text{C=O} \rightarrow \sigma^*$
Position [eV]	285.44	289.72	290.6	291.3	294.6	294	300.2	303.15
Width [eV]	2.95	4.72	1.0	1.0	1.0	22.80	22.00	22.10
Exp. decay	0.32	0.32	0.01	0.01	0.01	0.50	0.5	0.5

Supplemental Table 6: N1s Peak Assignments for PDIC+ED Chemistry

Assignment	$\text{N-C} \rightarrow \pi^*$	N-C Step	$\text{N-C} \rightarrow \sigma^*$
Position [eV]	402.7	404.68	407.74
Width [eV]	19.94	1	19.82
Exp. decay	0.1	0.017	0.550

Supplemental Table 7: Peak Assignments for PDIC+BD Chemistry

Assignment	$(\text{C-C})_{\text{ring}} \rightarrow \pi^*$	$\text{C=O} \rightarrow \pi^*$	C-C Step	$(\text{C-C})_{\text{ring}} \text{ Step}$	C-N Step	C=O Step	$\text{C-C} \rightarrow \sigma^*$	$\text{C-N} \rightarrow \sigma^*$	$\text{C=O} \rightarrow \sigma^*$
Position [eV]	285.575	289.87	290.1	290.6	291.1	294.6	293.59	300.05	304.63
Width [eV]	3.11	5.14	1	1	1	1	21.30	20.56	21.94
Exp. decay	0.3	0.32	0.01	0.01	0.01	0.01	0.5	0.5	0.5

Supplemental Table 8: N1s Peak Assignments for PDIC+BD Chemistry

Assignment	$\text{N-C} \rightarrow \pi^*$	N-C Step	$\text{N-C} \rightarrow \sigma^*$
Position [eV]	402.7	404.59	408.09
Width [eV]	20.32	1	20.44
Exp. decay	0.15	0.017	0.55

Supplemental Table 9: Peak Assignments for BDIC+ED Chemistry

Assignment	C=O \rightarrow π^*	C-C Step	C-N Step	C=O Step	C-C \rightarrow σ^*	C-N \rightarrow σ^*	C=O \rightarrow σ^*
Position [eV]	289.89	290.1	291.1	294.6	295.42	299.17	303.77
Width [eV]	4.72	1	1	1	15.18	15.62	13.30
Exp. decay	0.3	0.01	0.01	0.01	0.4	0.5	0.45

Supplemental Table 10: N1s Peak Assignments for BDIC+ED Chemistry

Assignment	N-C \rightarrow π^*	N-C Step	N-C \rightarrow σ^*
Position [eV]	402.7	406	408.82
Width [eV]	4.52	1	19.2
Exp. decay	0.017	0.017	0.6

Supplemental Table 11: Peak Assignments for BDIC+BD Chemistry

Assignment	C=O \rightarrow π^*	C-C Step	C-N Step	C=O Step	C-C \rightarrow σ^*	C-N \rightarrow σ^*	C=O \rightarrow σ^*
Position [eV]	289.9	290.1	291.1	294.6	295.32	299.07	303.55
Width [eV]	3.54	1	1	1	21.44	19.42	21.90
Exp. decay	0.3	0.004	0.004	0.01	0.4	0.4	0.4

Supplemental Table 12: N1s Peak Assignments for BDIC+BD Chemistry

Assignment	N-C \rightarrow π^*	N-C Step	N-C \rightarrow σ^*
Position [eV]	402.7	405.75	408.57
Width [eV]	8.52	1	19.2
Exp. decay	0.3	0.017	0.6

References

- (1) Loscutoff, P. P. W.; Zhou, H.; Clendenning, S. B. S. S. B.; Bent, S. F. S. Formation of organic nanoscale laminates and blends by molecular layer deposition. *ACS Nano* **2010**, *4*, 331–341 DOI: 10.1021/nn901013r.
- (2) Watts, B.; Swaraj, S.; Nordlund, D.; Lüning, J.; Ade, H. Calibrated NEXAFS spectra of common conjugated polymers. *J. Chem. Phys.* **2011**, *134*, 24702 DOI: 10.1063/1.3506636.
- (3) Urquhart, S. G.; Hitchcock, A. P.; Priester, R. D.; Rightor, E. G. Analysis of polyurethanes using core excitation spectroscopy. Part II: Inner shell spectra of ether, urea and carbamate model compounds. *J. Polym. Sci. Part B Polym. Phys.* **1995**, *33*, 1603–1620 DOI: 10.1002/polb.1995.090331105.
- (4) Hähner, G.; Kinzler, M.; Wöll, C.; Grunze, M.; Scheller, M. K.; Cederbaum, L. S. Near Edge X-Ray-Absorption Fine-Structure Determination of Alkyl-Chain Orientation: Breakdown of the “Building-Block” Scheme. *Phys. Rev. Lett.* **1992**, *69*, 694–694 DOI: 10.1103/PhysRevLett.69.694.
- (5) Fu, J.; Urquhart, S. G. Linear Dichroism in the X-ray Absorption Spectra of Linear n -Alkanes. *J. Phys. Chem. A* **2005**, *109*, 11724–11732 DOI: 10.1021/jp053016q.